Highly Aligned Lamellar Lipid Domains Induced by Macroscopic Confinement

M.-P. Nieh,[†] V. A. Raghunathan,[‡] H. Wang,[§] and J. Katsaras*,[†]

National Research Council, Steacie Institute for Molecular Sciences, Building 459, Stn. 18, Chalk River, Ontario, K0J 1J0, Canada, Raman Research Institute, Bangalore 560 080, India, and Materials Science and Engineering, Michigan Technological University, 504 M and ME Building, 1400 Townsend Drive, Houghton, Michigan 49931-1295

Received March 31, 2003. In Final Form: May 22, 2003

We have carried out neutron diffraction experiments on a lipid mixture in a macroscopically confined sample geometry (1 mm gap) and have observed the transformation of bilayered micelles into two distinct orientationally aligned domains of perforated lamellae seemingly littered with defects. Depending on the separation of the confining surfaces, the defects can lie on a two-dimensional centered rectangular lattice where the angle, ϕ, between lamellar domains can vary. The particular lamellar phase is shown to be metastable and eventually relaxes, either in time or by perturbation of the sample by centrifugation, into aligned multibilayer stacks of single orientation.

1. Introduction

There has been a great deal of interest in bilayered micelles (Figure 1a), often referred to as bicelles, composed of dimyristoyl phosphatidylcholine (DMPC), which consists of two 14-carbon-long saturated (no double bonds) hydrocarbon chains, and the short-chain lipid dihexanoyl phosphatidylcholine (DHPC, two 6-carbon-long saturated acyl chains).[1−6] The stability of these bilayered micelles is explained in terms of the preference of the short-chain DHPC lipid for regions of high curvature, which lowers the edge energy of the aggregates.

Previously it was thought that bicelles existed only at temperatures of >25 °C.[1−4,7,8] However, recent small-angle neutron scattering (SANS) studies showed that the bicelles were in fact found at temperatures below 25 °C and at T > 25 °C, they transformed into L_α phase lamellae.[5,9] These L_α bilayers, created from the coalescing bilayered micelles, are littered with pores whose edges are believed to be lined with short-chain DHPC molecules (Figure 1b).[5] To mimic biological membranes and prevent phase separation at high temperatures, often a negatively charged lipid like dimyristoyl phosphatidylglycerol (DMPG) is added to the DMPC/DHPC bicelle mixture. In the L_α phase, the DMPC/DHPC system has a negative diamagnetic anisotropy ($\Delta\chi$); however, on doping these samples with paramagnetic lanthanide ions (usually Tm^{3+} or Yb^{3+}), the sign of $\Delta\chi$ is reversed. As both the nondoped and lanthanide-doped systems can be aligned by an external magnetic field, they have become popular with nuclear magnetic resonance spectroscopists where they are used as "substrates" to align membrane-associated proteins.[2,10,11] Recently, partial phase diagrams of the lanthanide-doped DMPC/DHPC and DMPC/DHPC/DMPG systems have been reported by Nieh et al.[5,9]

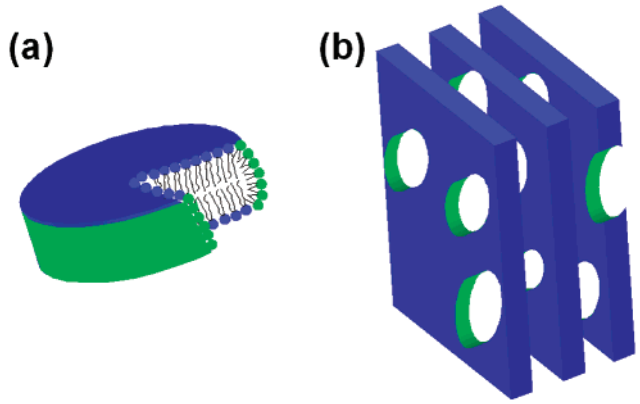

Figure 1. (a) Schematic drawing of a bilayered micelle or so-called bicelle composed of DMPC and DHPC lipid molecules. The short-chain DHPC lipid molecules (in green) occupy the rim of the bicelle, while the long-chain DMPC and DMPG lipids (in blue) are found on the major faces of the micelle. When the bicelles coalesce, the resultant structures are perforated extended lamellae (b) with DHPC molecules coating the pores.

Liquid crystalline materials can be influenced by the presence of nearby surfaces. In recent years, there have been experimental reports of complex fluids aligning under confinement and/or flow with distances between confining surfaces ranging from 0.4 to tens of microns.[12] Moreover, using a Landau−de Gennes approach, it has been shown that the so-called bookshelf smectic configuration, where the smectic layers arrange themselves in layers perpendicular to the confining surfaces, can experience a number of structural transformations.[13] One such structural

[†] National Research Council.
[‡] Raman Research Institute.
[§] Michigan Technological University.

(1) Sanders, C. R., II; Schwonek, J. P. *Biochemistry* **1992**, *31*, 8898.
(2) Sanders, C. R., II; Hare, B. J.; Howard, K. P.; Prestegard, J. H. *Prog. NMR Spectrosc.* **1994**, *26*, 421.
(3) Katsaras, J.; Donaberger, R. L.; Swainson, I. P.; Tennant, D. C.; Tun, Z.; Vold, R. R.; Prosser, R. S. *Phys. Rev. Lett.* **1997**, *78*, 899.
(4) Tjandra, N.; Bax, A. *Science* **1997**, *278*, 1111.
(5) Nieh, M.-P.; Glinka, C. J.; Kruger, S.; Prosser, R. S.; Katsaras, J. *Langmuir* **2001**, *17*, 2629.
(6) Faham, S.; Bowie, J. U. *J. Mol. Biol.* **2002**, *316*, 1.
(7) Sanders, C. R.; Prosser, R. S. *Structure* **1998**, *6*, 1227.
(8) Arnold, A.; Labrot, T.; Oda, R.; Dufourc, E. J. *Biophys. J.* **2002**, *83*, 2667.
(9) Nieh, M.-P.; Glinka, C. J.; Kruger, S.; Prosser, R. S.; Katsaras, J. *Biophys. J.* **2002**, *82*, 2487.
(10) Vold, R. R.; Prosser, R. S. *J. Magn. Reson., Ser. B* **1996**, *113*, 267.
(11) Vold, R. R.; Prosser, R. S.; Deese, A. J. *J. Biomol. NMR* **1997**, *9*, 329.
(12) Koltover, I.; Idziak, S. H. J.; Davidson, P.; Li, Y.; Safinya, C. R.; Ruths, M.; Steinberg, S.; Israelachvili, J. N. *J. Phys. II* (*France*) **1996**, *6*, 893.

10.1021/la034549y CCC: $25.00
Published on Web 07/12/2003

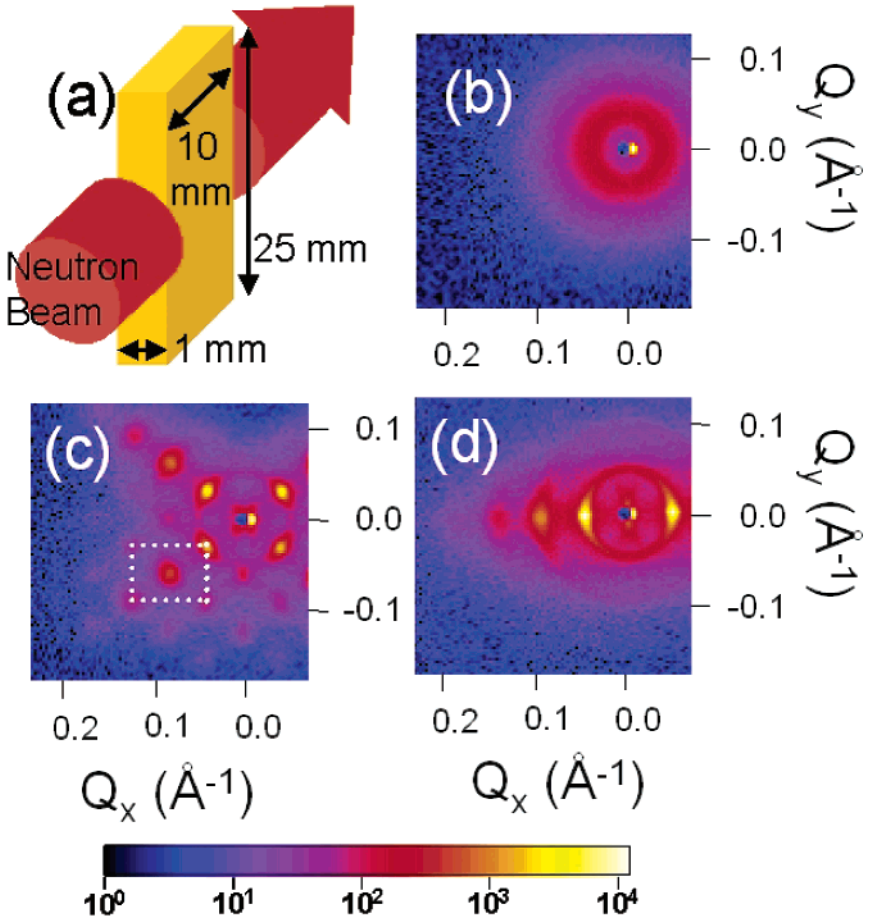

Figure 2. (a) Scattering geometry of the incident neutron beam relative to the quartz cuvette. (b) Two-dimensional diffraction pattern obtained at 10 °C, from an isotropic micellar solution. (c) 2D diffraction pattern obtained at 35 °C, corresponding to two orientationally distinct lamellar domains (d = 131 Å) giving rise to the X-pattern and weak satellite peaks due to a centered rectangular lattice (shown as dotted lines) with a = 157 Å and b = 209 Å. (d) Diffraction pattern obtained on centrifuging the sample at 35 °C, arising from an aligned lamellar phase with d = 131 Å. The lamellae are aligned with their bilayer normals perpendicular to the 10 mm face of the sample cell. The false color scale is logarithmic.

change is the buckled chevron state where the smectic layers form a V-shape. Nevertheless, it is generally accepted that when the confining surfaces contain a gap of fractions of a millimeter or greater, the influence of the nearby surfaces on the liquid crystalline material is at best minimal.

Here we report the transformation of bilayered micelles in the biomimetic DMPC/DHPC/DMPG/water system into two distinct orientationally aligned domains of perforated lamellae whose interfaces are seemingly populated with defects. Moreover, the defects lie on a 2D centered rectangular lattice. The phase is formed via a rapid increase in temperature, and the alignment is imparted solely by macroscopic confinement (1 mm separation of the confining surfaces). The induced phase is shown to be metastable and relaxes, either in time or by perturbation of the sample by centrifugation, into singly oriented aligned multibilayer stacks with the plane of the bilayers lying parallel to the major faces of the quartz confining surfaces. To the best of our knowledge, this system is unique in that it aligns in macroscopic gaps of up to 5 mm.

2. Materials and Experimental Methods

DMPC, DHPC, and DMPG were purchased from Avanti Polar Lipids (Alabaster, AL) and were used without any further purification. The samples were prepared by vortexing appropriate amounts of the lipids in D_2O (99.9%, Cambridge Isotope Co.) until a homogeneous dispersion was obtained. The total lipid concentration was 25 wt %, and the molar ratios of DHPC/DMPC and of DMPG/DMPC were 0.2 and 0.067, respectively. For SANS experiments, the samples were taken up in quartz cells with the following rectangular cross section (neglecting height): (a) 2 mm × 0.2 mm; (b) 10 mm × 1 mm; (c) 10 mm × 5 mm. (d) For the 2 mm gap experiments, a "banjo" type quartz cell of radius 12.7 mm was used. SANS experiments were carried out on the NG7 30m and NG1 8m SANS instruments, equipped with two-dimensional detectors, at the Center for Neutron Research (NIST, Gaithersburg, MD). The wavelength of neutrons used was 5.0 Å with a wavelength spread ($\Delta\lambda/\lambda$) of 11% for NG7 and 20% for NG1. The scattering geometry was such that the 12.7 mm diameter neutron beam was parallel to the major surfaces (10 mm × 25 mm) of the sample cell (Figure 2a). The sample-to-detector distances were 2 and 3.6 m for NG7 and NG1, respectively. The accessible range of the scattering vector, Q ($4\pi \sin(\theta/2)/\lambda$), was from 0.01 to 0.25 Å^{-1}. θ is the scattering angle. As a result of the neutron beam size, which effectively bathed the entire sample, and the large $\Delta\lambda/\lambda$, the diffraction patterns were collected without the need to rotate the sample.

3. Results and Discussion

The diffraction pattern obtained at 10 °C, using a quartz sample cell with a 1 mm gap, shows one diffuse ring (Figure 2b) with no preferred orientation corresponding to the isotropic bilayered micellar phase (Figure 1a). From analysis of the scattered intensity, the aggregates in this phase are found to have a disklike shape of radius ~ 200

(13) Slavinec, M.; Kralj, S.; Žumer, S.; Sluckin, T. J. *Phys. Rev. E* **2001**, *63*, 031705-1.

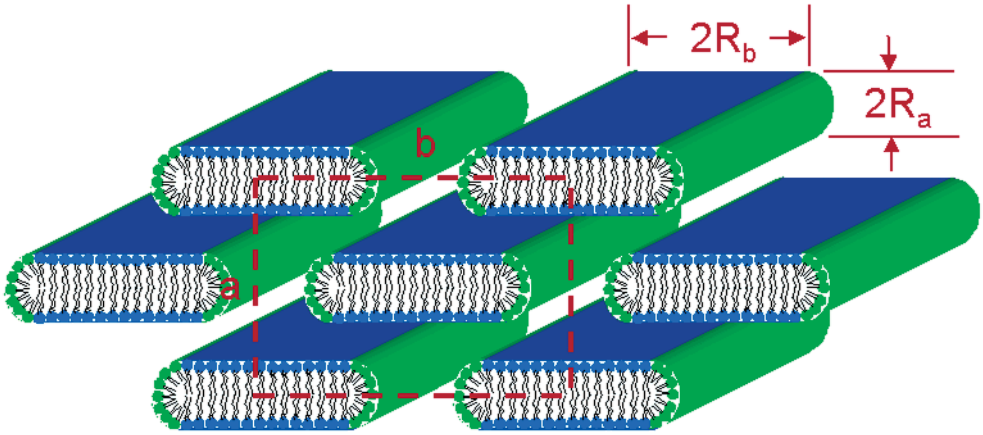

Figure 3. A schematic of the ribbonlike aggregates arranged on a two-dimensional centered rectangular lattice. In this direct ribbon phase, the hydrophilic headgroups of the amphiphilic molecules are on the surface of the ribbons while the hydrophobic hydrocarbon chains are sequestered inside. a and b represent the 2D lattice parameters while $2R_a$ and $2R_b$ are the ribbon's thickness and width, respectively (Appendix). The DMPC and DHPC lipid molecules are colored blue and green, respectively.

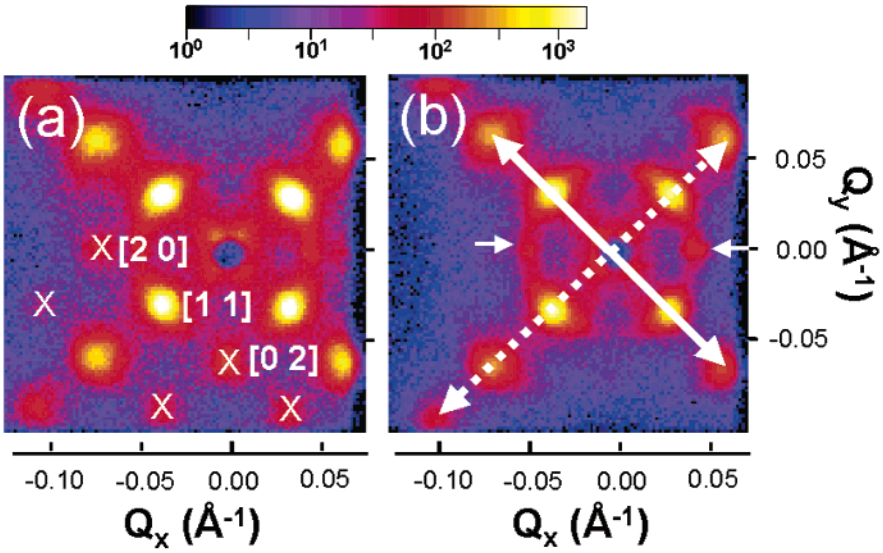

Figure 4. (a) 2D diffraction pattern, obtained at 40 °C via a rapid increase in temperature, showing the distinct X-pattern and weak satellite reflections (indicated by the white × symbols). The Miller indices are given for three reflections assuming a centered-rectangular lattice. (b) 2D pattern of the same sample after cycling between 40 and 0 °C. The weak satellite reflections are no longer observable, while the X-pattern remained unaltered. The temperature was 40 °C. The bidirectional solid and dashed arrows depict the family of reflections due to the two distinct lamellar domains. The small arrows at $Q_y = 0$ are the result of a small population of lamellae, probably in direct contact with the confining surfaces, whose bilayer normals are perpendicular to the confining surface. All lamellar reflections have the same d.

Å and thickness ∼ 40 Å .[5] On raising the temperature to 35 °C, the viscosity of the sample increases dramatically, forming a gel, indicative of the formation of large aggregates. Moreover, the diffuse ring in the diffraction pattern is replaced by a set of Bragg spots (Figure 2c). To produce these diffraction patterns, the sample must be well aligned, with large domains that span the width of the sample cell (1 mm) as the 12.7 mm diameter incident beam completely bathed the sample with neutrons. These well-aligned samples were obtained on heating at a rate of 1 °C/min from the micellar phase, whereas slower heating (∼1 °C/h) led to poorly oriented samples with the same Bragg spots in Figure 2c being smeared out over 2π. Besides alignment, we do not expect any other differences between the two heat treatments.

Rotating the sample by 90° (the incident neutron beam is now perpendicular to the 10 mm major face, 1 mm path length) usually yielded a diffraction pattern consisting of the four most intense reflections seen in Figure 2c and superposed on a powder pattern of the same lamellar periodicity (data not shown). This implies that the alignment imposed by the 1 mm cell surfaces is weak.

The diffraction pattern of the intermediate phase (Figure 2c) can be indexed on a 2D centered rectangular lattice with $a = 157$ Å and $b = 209$ Å, corresponding to the space group cmm. Interestingly, this pattern remains unchanged even at temperatures approaching 90 °C. However, if the sample is disturbed, as for example by centrifugation, the diffraction pattern changes drastically to that of a well-aligned lamellar phase (Figure 2d) with a repeat spacing $d = 131$ Å. Furthermore, on leaving the sample undisturbed at 35 °C, we found the rectangular phase to relax into the aligned lamellar phase over a period of a few weeks (data similar to Figure 2d). This is direct evidence that the structural phase giving rise to the diffraction pattern in Figure 2c is metastable.

Upon first examination, the distinct presence of a centered rectangular lattice is reminiscent of ribbonlike

aggregates (Figure 3) which have, on occasion, been found between the hexagonal and lamellar phases in aqueous solutions of surfactants (amphiphilic molecules that usually contain only one hydrocarbon chain).[14−17] However, we were unable to fit the ribbon phase to the neutron scattering intensity distribution shown in Figure 2c (see Appendix). It is interesting to note that the diffraction pattern in Figure 2c is characterized by two sets of intense reflections, forming an X, and a set of much weaker "satellite" reflections. If the ribbon phase was indeed present, some of the satellite peaks would be much more intense. Moreover, although the intensity ratios of the strong reflections defining the X-pattern were for the most part constant, this could not be said for the satellite peaks whose intensities varied considerably from sample to sample and in some cases were experimentally not observable. In our case, the existence of ribbons, even as a minor phase, is thus negated on the following criteria: (a) The amount of DHPC in the system is not sufficient to make ribbons of the requisite dimensions.[18] (b) Ribbons have previously only been seen in molecules containing only one hydrocarbon chain and sandwiched between hexagonal and lamellar phases.[14−17] (c) The observation of a pure ribbon phase was never observed even when carrying out fine temperature scans. (d) Most importantly, we were unable to fit the diffracted intensities to the ribbon model (Figure 3). The buckled chevron state, mentioned previously, is also excluded as a possible structure as its diffraction pattern would not contain the satellite peaks forming a 2D centered rectangular lattice.

The 2D diffraction pattern, from a different sample preparation from that in Figure 2, is shown in Figure 4a and is indistinguishable from the pattern shown in Figure 2c. However, after cycling between 40 and 0 °C the so-called satellite peaks seen in Figure 4a (indicated by Xs) were no longer visible (Figure 4b). *Thus it is clear that the structural phase in Figures 2c and 4a is defined only by the reflections making up the X-pattern and not the weak satellite reflections.* Also, the diffraction patterns in Figure 4 contain two relatively weak reflections along Q_x and happen to fall on the same "powder" ring as the four most intense reflections forming the X-pattern. Moreover, the repeat spacing of the powder ring is practically the same ($d = 125$ Å) as the lamellar repeat spacing of the aligned lamellae in Figure 2d.

Taking all of the above-mentioned information into account, we present a schematic of the structural phase giving rise to the diffraction patterns in Figures 2c and 4. The phase basically consists of two orientationally distinct lamellar domains making an angle ϕ. The distinct X-pattern in Figures 2c and 4 is the direct result of these two highly aligned lamellar domains. Of significance is that the lamellar domains contributing to the X-pattern have similar lamellar repeat spacings as the stable uniorientational lamellar bilayers giving rise to the pattern in Figure 2d. To further make the case for the existence of two orientationally distinct lamellar domains, we present the following evidence: (a) The structure factor amplitude ratios of the lamellar peaks in Figure 2d are

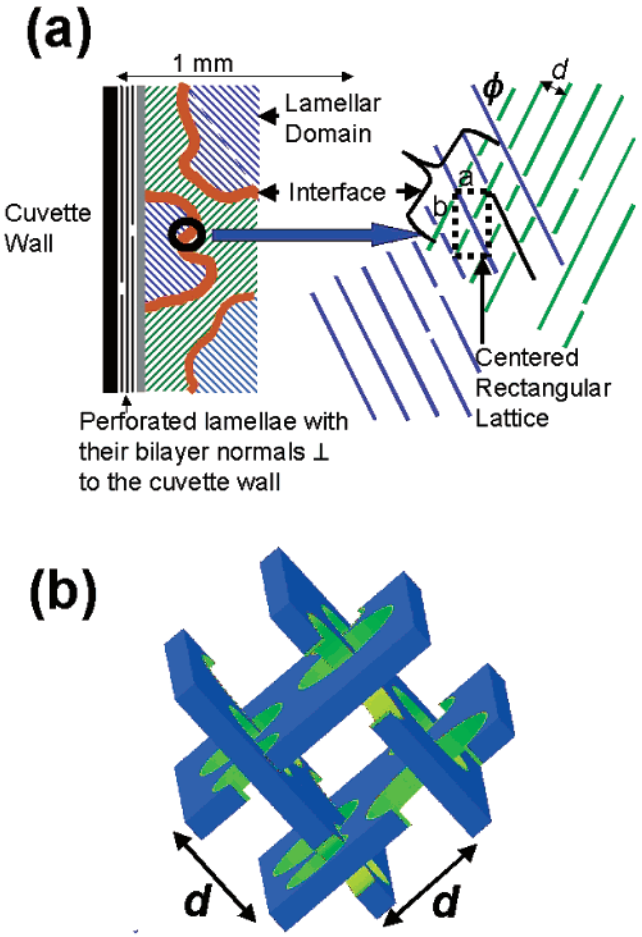

Figure 5. (a) Schematic of the confined geometry and the proposed structural phase containing two orientationally distinct lamellae making an angle ϕ. The defects are formed at the interface between the two domains of lamellae and reside on a centered rectangular lattice, as depicted by the dashed lines, whose lattice constants are given by a and b. d is the lamellar repeat spacing. A small fraction of lamellae are aligned with their bilayer normals perpendicular to the wall of the sample cell, consistent with the data in Figure 2. The gray region depicts the interface between these lamellae and those that are tilted with respect to the sample cell's major faces. (b) 3D schematic of the interface region showing the defects and the relationship between the two lamellar orientations.

practically indistinguishable from those same ratios along either arm of the X-patterns in Figures 2c[19] and 4, implying that the structures giving rise to the diffraction patterns are equivalent. (b) Diluting the system in Figure 2c with D_2O resulted in 1D swelling (data not shown), indicative of the presence of extended lamellar sheets.[20] A ribbon or hexagonal phase, for example, would exhibit 2D swelling.

If the X-patterns (Figures 2c and 4) are the direct result of lamellar domains present in two distinct orientations and making an angle ϕ with respect to each other, then what gives rise to the weak satellite peaks (Figures 2c

(14) Kékicheff, P.; Cabane, B. *J. Phys.* (*Paris*) **1987**, *48*, 1571.
(15) Hendrikx, Y.; Charvolin, J. *J. Phys.* (*Paris*) **1981**, *42*, 1427.
(16) Chidichimo, G.; Vaz, N. A. P.; Yaniv, Z.; Doane, J. W. *Phys. Rev. Lett.* **1982**, *49*, 1950.
(17) Hagslatt, H.; Söderman, O.; Jönsson, B. *Liq. Cryst.* **1994**, *17*, 157.
(18) Using the largest possible ribbons [40 Å (bilayer thickness) by 200 Å (width of ribbon)] and assuming that all of the short-chain DHPC lipids and long-chain DMPC lipids are located at the ribbon's high curvature and low curvature regions, respectively, we calculate the molar ratio of DMPC/DHPC to be ≈3.2. This is much different than the experimentally used DMPC/DHPC ratio of 5.
(19) The structure factor amplitude ratios of the first- to second-order peaks, S_1/S_2, and of the second- to third-order peaks, S_2/S_3, for the lamellar phase in Figure 2d are 2.1 and 2.2, respectively. The same structure factor ratios for the two orientationally distinct lamellar phases (Figure 2c) yielded $S_1/S_2 = 1.9$ and $S_2/S_3 = 2.1$. This is good proof for the existence of a lamellar phase in Figure 2c.
(20) For 1D swelling, the peak position, Q_{max}, is proportional to the total lipid concentration, c. Lamellar structures are representative of 1D swelling. On the assumption that the object size remains invariant as a function of c, cylinders such as hexagonal and ribbon phases exhibit 2D swelling ($Q_{max} \sim c^{1/2}$) while 3D swelling is characteristic of particles such as spheres, disks, etc. ($Q_{max} \sim c^{1/3}$).

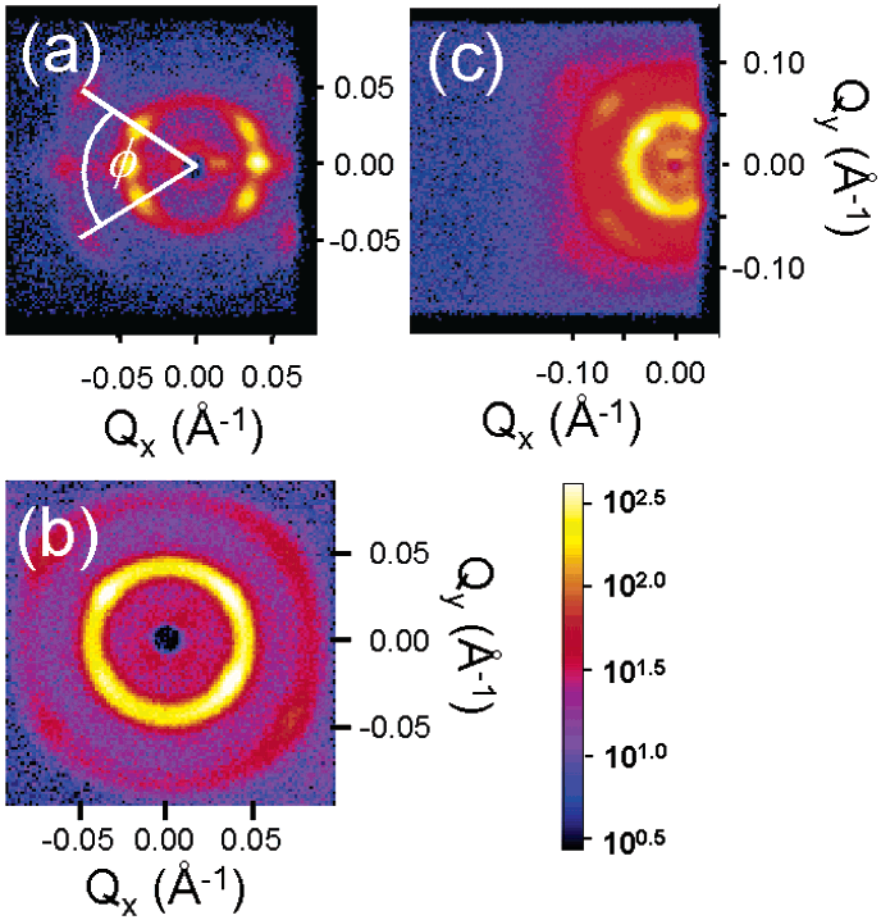

Figure 6. 2D diffraction patterns as a function of gap size at 40 °C. (a) 0.2 mm gap showing the presence of three distinct lamellar orientations. (b) The formation, in a 2 mm gap, of a smeared-out X-pattern. (c) Further deterioration of the alignment of the phase in a gap of 5 mm. The angle ϕ made by two orientationally distinct lamellar domains is 65° for a gap of 0.2 mm and 80° for all other gap sizes. The d values for 0.2, 2.0, and 5.0 mm gap sizes were 139, 125, and 128 Å, respectively. The error in d is ±5 Å. All of these phases are metastable, similar to the one in Figure 2c.

and 4a)? Evidence as to their origin can be found in Figure 4. As mentioned previously, the diffraction pattern in Figure 4a was obtained from a sample practically indistinguishable from the one in Figure 2c. Once formed, the sample was temperature cycled between 40 and 0 °C and the weak satellite peaks seen in Figure 4a (indicated by Xs) disappeared (Figure 4b). The structure factor amplitude ratios of the lamellar peaks giving rise to the X-pattern were unaltered after temperature cycling (Figure 4). A plausible explanation is that the weak satellite reflections (Figures 2c and 4a) are the result of defects occurring at the interfaces of the two different orientated lamellar domains. Moreover, these defects lie on a 2D centered rectangular lattice which, we believe, is formed concurrently with the lamellar domains, thus resulting in some of the 2D centered rectangular reflections overlapping with the reflections from the lamellar domains, that is, the reflections forming the X-pattern. More precisely, we define a defect as part of a lipid bilayer from one orientation penetrating, through a pore, a lipid bilayer from another orientation (Figure 5). Even in the case where the defect lattice is not observed (Figure 4b), the defects themselves are most likely present, still residing on a 2D lattice, but not seen because (a) the number of defects varies considerably from sample to sample and (b) misalignment of the lamellar domains smears out the already weak intensity maxima.

Figure 5 is a schematic of the structural phase made up of two orientationally distinct lamellar phases whose interfaces are seemingly littered with defects lying on a 2D lattice. This structure adequately accounts for all of the features present in the data (Figures 2c and 4). The major sample cell surfaces, most likely, are coated with a few bilayers whose normals are perpendicular to the major surface (Figure 5a) and whose presence is deduced from the data present in Figure 4.

Starting from the low-temperature phase (10 °C), it thus seems that with increasing temperature bilayered micelles coalesce, forming perforated lamellar stacks (Figure 1).[5,9] It is reasonable to assume that at the earliest stage of coalescing bicelles, intermediate size perforated lamellae come into existence with the pores "trapping" either other lamellae or individual bicelles. At the same time, the trapped lamellae or bicelles grow through more coalescing with the end result being the insertion of part of a lamella, from one orientation, into the perforation of the lamella in the other orientation thus "locking" the domains into the two distinct lamellar orientations (Figure 5b). This interpenetration between bilayer domains spans a number of bilayers (correlation length) giving rise to distinct Bragg reflections. The perforations along the lamellae are not positionally correlated and do not have to form elongated "gashes". The surface charge imparted by the DMPG lipid molecules in conjunction with the confinement gap dictates the orientation, ϕ, between the two orientational lamellar domains. Upon annealing-out the defects, either through time (days to weeks) or mechanical means, the bilayers relax to their stable configuration of lamellae (Figure 2d) which have the same d as the metastable lamellar stacks (Figure 2c).

Experiments using the same temperature protocol to obtain the metastable lamellar phase (Figure 2c) but with gap sizes other than 1 mm are presented in Figure 6. Figure 6a shows the diffraction pattern obtained from a sample with gap geometry of only 0.2 mm. $\phi = 65°$, instead of $\approx 80°$ seen in the other gap geometries (Figures 2c and 6b,c), is observed. Although there is no indication of a two-dimensional distribution of defects, as seen in Figures 2c and 4a, the Bragg peaks along Q_x (Figure 6a) are indicative of a lamellar phase whose bilayer normals are perpendicular to the confining surfaces and similar to the stable lamellar phase in Figure 2d and the data in Figure 4. d is identical for all three orientations of lamellae (Figure 6a); that is, they all lie on the same Bragg ring. We also believe that further decreasing the gap size ($\ll 0.2$ mm) will probably result in a single population of lamellae with their bilayer normals perpendicular to the confining surface.

Increasing the gap size causes ϕ to reach a limiting value of $\approx 80°$. We speculate that in the absence of confinement the induced charge on the lamellar surface, imparted by DMPG lipid molecules, will repel the two orientationally distinct lamellae up to a maximum of $\phi = 90°$. However, because of the confining surfaces, this maximum ϕ value is never realized. Bilayers whose normals are perpendicular to the confining sample cell surfaces (Figure 6a) are not present in amounts capable of contributing to a significant signal (Figure 6b,c). Moreover, the alignment of the two lamellar domains is poor (as judged by the presence of powder diffraction rings with nonuniform intensities), and no satellite peaks are observed as a result of defects lying on a 2D lattice (Figure 6b,c). It thus seems that only when the size of the gap is 1 mm are conditions such that the two orientational lamellar domains highly align, forming significant amounts of regularly spaced defects.

Theoretical studies show the possibility of different defect configurations in the L_α phase of amphiphile/water systems.[21] One of them is a stripelike pattern of parallel channels in the bilayers. In principle, it is possible for these channels in different bilayers to align in such a way as to form a 2D lattice, similar to the three-dimensional lattice of pores reported in lipid bilayers containing certain antimicrobial peptides.[22] The forces stabilizing this defect lattice can be expected to be weak, and hence this structure would be fragile and small external perturbations would destroy the long-range order of the channels. Since such a defect lattice can also give rise to a diffraction pattern as pictured in Figures 2c and 4a, we have considered this possibility. However, the fact that neither of the lattice parameters, a or b, is equal to twice the lamellar spacing (Figure 2d) rules out this possibility.

4. Concluding Remarks

In conclusion, we have presented evidence for the existence of two orientationally distinct lamellar domains whose interfaces are seemingly populated with defects lying on a 2D centered rectangular lattice. The interplay between the net charge of the system and the gap of the confining surfaces dictates the degree of alignment. This phase is shown to be metastable and relaxes, either in time or by perturbation of the sample by centrifugation, into aligned multibilayer stacks of single orientation. Of special interest is that the present system can be induced by confinement effects to form highly aligned lamellar domains spanning the entire 1 mm width of the sample cell, something that, to the best of our knowledge, has not been previously reported.

Acknowledgment. We thank Thad A. Harroun and Charles J. Glinka for their careful reading of the manuscript and helpful comments. We also thank the National Institute of Standards and Technology, U.S. Department of Commerce, for providing us with neutron beamtime to carry out the experiments reported here.

5. Appendix

The diffraction pattern of aligned ribbons (Figure 3) lying on a 2D centered rectangular lattice with their bilayer normals perpendicular to the confining wall surface can be simulated as follows: The rectangular ribbons are assumed to be identical to each other with uniform density and perfectly aligned throughout the entire sample. The intensity of a Bragg reflection is proportional to the product of the form factor, $P(Q)$, of a single ribbon and the structure factor, F_{hk}, for a 2D centered rectangular lattice, where h and k are the Miller indices.

$P(Q)$ for a ribbon can be derived from the Fourier transform of the spatial density function, $\rho(\mathbf{r})$, as follows:

$$P(\mathbf{Q}) = \left(\int \rho(\mathbf{r}) e^{i\mathbf{Q}\cdot\mathbf{r}}\, d\mathbf{r}\right)^2$$

Let $\mathbf{Q} = \mathbf{Q}_{||} + \mathbf{Q}_\perp$, where $\mathbf{Q}_{||}$ is the component of $\mathbf{Q}$ along the ribbon axis (z-axis) and $\mathbf{Q}_\perp$ is in the $x-y$ plane.

$$\begin{aligned} P(\mathbf{Q}) &= \left(e^{i\mathbf{Q}_{||}\cdot\mathbf{z}}\, dz \int \rho(\mathbf{r}_\perp) e^{i\mathbf{Q}_\perp\cdot\mathbf{r}_\perp}\, d\mathbf{r}_\perp\right)^2 \\ &= \left(\rho\delta(Q_{||}) \int_{-R_a}^{R_a} e^{iQ_x x}\, dx \int_{-R_b}^{R_b} e^{iQ_y y}\, dy\right)^2 \\ &= \left(\rho\delta(Q_{||})\right)^2 \left(\frac{2R_a \sin(Q_x R_a)}{(Q_x R_a)} \frac{2R_b \sin(Q_y R_b)}{(Q_y R_b)}\right)^2 \end{aligned}$$

where $2R_a$ is the ribbon thickness and $2R_b$ is the width of the ribbon. F_{hk} is a constant for $(h + k)$ even reflections and 0 for $(h + k)$ odd reflections. Since the scattered intensity $I(Q)$ for perfectly aligned ribbons on a 2D centered rectangular lattice can be expressed as the product of $P(Q)$ and F_{hk}, $I(Q)$ is nonzero only at locations where Bragg peaks occur (i.e., where $Q_x = 2\pi h/a$ and $Q_y = 2\pi k/b$ and $(h + k)$ results in an even number, except 0).

From our experimental results, we unambiguously determined the unit cell and its lattice parameters ($a = 157$ Å and $b = 209$ Å). The thickness of DMPC bilayers ($2R_a$) is approximately 35 Å. The only variable is the width of the ribbons, $2R_b$, which we expect to lie somewhere between 35 Å, the bilayer thickness, and the unit cell dimension b. The observed intensity ratio for the (11) and (20) reflections is 14. The calculated ratio for $2R_b = 35$ Å is 1.6 and for $2R_b = 200$ Å is 0.006. This result nullifies the possibility that our system is forming ribbons.

LA034549Y

(21) Bagdassarian, C. K.; Roux, D.; Ben-Shaul, A.; Gelbart, W. M. *J. Chem. Phys.* **1991**, *94*, 3030.

(22) Yang, L.; Weiss, T. M.; Lehrer, R. I.; Huang, H. W. *Biophys. J.* **2000**, *79*, 2002.